

**FABRICATION AND CHARACTERIZATION OF GaN
GROWN ON CUBIC Si (100) AND GaAs (001)
SUBSTRATES**

by

SITI NURUL WAHEEDA BINTI MOHMAD ZAINI

**Thesis submitted in fulfilment of the requirements
for the degree of
Master of Science**

September 2015

ACKNOWLEDGEMENT

To begin with, let me praise upon Allah for the courage and spirit given to me in accomplishing my thesis successfully. I am also honoured to express my deepest appreciation to my supervisor Dr Norzaini Zainal for giving me a chance to be a part of her research team besides her encouraged attitude with continuous guidance, motivation and patience throughout my years as a master student. Without her help and support, this thesis is impossible to be completed.

Besides, I would like to thank Malaysian Ministry of Education for the MyBrain15 scholarship programme that provides me with some financial support during my study.

It is grateful to have such colleagues like Ezzah, Esmed, Ikram, Azharul and Alvin, for being helpful and great buddies. Special thanks to Ikram and Alvin for your assistance in capturing FESEM images of my samples. Not forgotten, for the time spent by Esmed and Azharul in helping me with the XRD measurements.

I would like to acknowledge all staffs, especially Nano-Optoelectronic Research and Laboratory (NOR lab) for their technical helps.

To my beloved parents, Siti Aishah Mohd Desa and Muhammad Azeem Rafique and also my dear siblings, Anin and Ejad this dissertation is dedicated to all of you and thanks for your love and support.

TABLES OF CONTENTS

	Page
ACKNOWLEDGEMENT.....	ii
TABLES OF CONTENTS.....	iii
LIST OF TABLES.....	v
LIST OF FIGURES.....	vi
LIST OF SYMBOLS.....	x
LIST OF ABBREVIATIONS.....	xii
LIST OF PUBLICATIONS.....	xiii
ABSTRAK	xiv
ABSTRACT	xvi
CHAPTER 1 : INTRODUCTION.....	1
CHAPTER 2 : THEORY AND LITERATURE REVIEW.....	5
2.1: Introduction to GaN material.....	5
2.2: Basic properties of GaN material.....	6
2.3: Type of defects exist in the growth of GaN material.....	8
2.4: Progress on GaN epitaxy.....	14
2.5: Thermal annealing treatment on GaN.....	16
2.6: Background study of porous fabrication on GaN layer.....	18
2.7: Progress on the growth of cubic GaN.....	20
2.8: Summary.....	24
CHAPTER 3 : EXPERIMENTAL PROCEDURES AND TECHNIQUES.....	26
3.1: Samples preparations and fabrications.....	26

3.2: Sample characterizations.....	31
3.3: Summary.....	45
CHAPTER 4 : RESULTS AND DISCUSSIONS.....	46
4.1: Characterizations of GaN layer grown on cubic Si (100) substrate.....	46
4.2: Effects of thermal annealing on GaN layer grown on Si (100) substrate.....	56
4.3: Fabrication of porous structure on GaN layer grown on Si (100) substrate.....	64
4.4: Effect of thermal annealing treatment on porous GaN/GaN grown on Si (100) substrate.....	66
4.5: Cubic GaN layers grown on GaAs (001) substrate.....	77
4.6: Summary.....	89
CHAPTER 5 : CONCLUSIONS AND FUTURE WORKS.....	91
REFERENCES.....	93

LIST OF TABLES

		Page
Table 2.1:	Basic properties of both hexagonal and cubic GaN	7
Table 2.2:	Comparison of the growth of GaN on different buffer layer and substrate.	15
Table 2.3:	Summary of some published works on annealing GaN at various temperature.	17
Table 2.4:	Data from published works on the crystalline quality and stress relaxation by the fabrication of the porous GaN prepared by different conditions.	19
Table 2.5:	Growth parameters used for growing cubic GaN layers by various groups.	21
Table 2.6:	Hexagonal inclusions in cubic GaN grown by different technique.	23
Table 3.1:	Peaks of Raman modes in hexagonal and cubic GaN structure with corresponding expected wavenumber, refers to [74,75].	40
Table 4.1:	FWHM of E ₂ (high) peak of GaN layers at different annealing temperature.	63
Table 4.2:	Average surface roughness and pore depth of porous GaN at different annealing conditions.	70
Table 4.3:	Calculated strain and stress for the GaN samples grown on Si substrate with different conditions.	74
Table 4.4:	Summarized data of Hall effect measurement of cubic GaN samples grown at different thickness.	90

LIST OF FIGURES

	Page
Figure 2.1: The atomic arrangement in hexagonal (wurtzite) and cubic (zinc-blende) GaN materials.	5
Figure 2.2: Stacking sequence of (a) hexagonal and (b) cubic lattice.	6
Figure 2.3: Mechanism of edge and screw dislocations in a semiconductor material [15].	9
Figure 2.4: The disrupted sequence in the stacking fault phenomenon.	10
Figure 2.5: Illustration of vacancy and substitutional defects in lattice structure.	11
Figure 2.6: Illustration of deformation of the object under an applied force [19].	12
Figure 2.7: Illustration of lattice matched and lattice mismatched mechanism in epitaxy.	13
Figure 3.1: Flow chart of working progress on GaN layers grown on different cubic substrates.	26
Figure 3.2: Schematic diagram of the thermal annealing setup.	27
Figure 3.3: Schematic diagram of the electrochemical etching setup to produce porous GaN on the GaN/Si (100) substrate.	28
Figure 3.4: Schematic diagram of field emission scanning electron microscopy (FESEM) measurement taken from [70].	30
Figure 3.5: Schematic diagram of tapping mode AFM measurement used in our work.	32
Figure 3.6: X-ray diffraction in a crystal lattice planes. The diagram has been modified from [71].	33
Figure 3.7: Expected peaks from the GaN sample reported by [47].	34
Figure 3.8: XRD phase analysis basic principle.	35
Figure 3.9: Schematic diagram of PL system used at Universiti Sains Malaysia.	37

Figure 3.10:	PL spectra of (a) hexagonal GaN/ Al ₂ O ₃ and (b) cubic GaN/GaAs samples, taken from [70].	38
Figure 3.11:	Optical phonon modes in atomic lattice of wurtzite structure.	39
Figure 3.12:	Raman spectra of GaN grown on GaAs substrate, this figure is taken from [76].	40
Figure 3.13:	A prism spectrograph diagram shows how monochromatic light has been dispersed into different wavelength. This drawing was taken from [77].	41
Figure 3.14:	A schematic diagram of Hall effect measurement. The inset figure (bottom right) shows the connection of the Hall voltage across the points with respect to the variation of current and the magnetic field (Van der Pauw method).	43
Figure 3.15:	Result taken from the Hall effect measurement.	44
Figure 4.1:	FESEM images of GaN on Si (100) substrate taken at different magnification (a) 5000x and (b) 50000x.	46
Figure 4.2:	(a) 2-D image and (b) 3-D image of GaN on Si (100) substrate taken by AFM measurement.	47
Figure 4.3:	XRD phase analysis of GaN sample grown on Si (100) substrate.	49
Figure 4.4:	XRD reciprocal space mapping (RSM) of (a) symmetric (002) and (b) asymmetric (-105) scans of GaN grown on Si (100) substrate.	50
Figure 4.5:	XRD rocking curve of (a) symmetric (002) scan and (b) asymmetric (102) scan of GaN grown on Si (100) substrate.	51
Figure 4.6:	(a) Room-temperature (300K) and (b) low-temperature (4 K) PL spectra of GaN grown on Si (100) substrate. The dashed line in the inset figure shows the Gaussian fitting to the measured data.	53
Figure 4.7:	Dependence of energy emission of GaN grown on Si (100) substrate on temperature.	54
Figure 4.8:	Raman spectrum of GaN grown on Si (100) substrate.	56
Figure 4.9:	FE-SEM images of GaN sample annealed at different annealing temperature of (a) non-annealed, (b) 600 °C, (c) 800 °C and (d) 1000 °C.	58

Figure 4.10:	Surface roughness average values of GaN samples at different annealing temperature. The inset figure represents the 3-D AFM images of the samples.	59
Figure 4.11:	XRD data on FWHM of the GaN samples annealed at different annealing temperature, as measured from (002) and (102) scans.	60
Figure 4.12:	PL spectra of GaN grown on Si (100) substrate annealed at different annealing temperature. The inset figure is the magnified PL spectra.	62
Figure 4.13:	Raman spectra of GaN samples with different annealing temperature, conducted at 300 K.	63
Figure 4.14:	A brief description on the framework proposed of making porous GaN layer grown on Si substrate.	64
Figure 4.15:	FESEM images of porous structure with different conditions.	66
Figure 4.16:	FE-SEM images of the porous GaN/GaN grown on Si (100) substrate (a) without annealing, (b) 800 °C post-annealing and (c) 800 °C pre-annealing GaN.	68
Figure 4.17:	AFM 3-dimensional (3D) images of porous GaN/GaN grown on Si (100) substrate of (a) without annealing, (b) 800 °C post-annealing and (c) 800 °C pre-annealing.	69
Figure 4.18:	XRD rocking curve of the porous GaN/GaN grown on Si (100) substrate of (a) without annealing (b) 800 °C post-annealing and (c) 800 °C pre-annealing.	72
Figure 4.19:	(a) Lattice constant and (b) strain level in c- and a- axis of different type of GaN samples grown on Si substrate.	73
Figure 4.20:	PL spectrum of the porous structure of (a) without annealing (b) post-annealing and (c) pre-annealing porous GaN grown on Si (100) substrate, conducted at 300 K.	75
Figure 4.21:	Dependence of PL band-edge energy on strain, ϵ_{zz} for (a) non-porous GaN, (b) non-annealed porous GaN and (c) pre-annealed porous GaN.	76
Figure 4.22:	Raman spectrum of the porous structure of (a) without annealing (b) post-annealing and (c) pre-annealing porous GaN grown on Si (100) substrate.	77

Figure 4.23:	(a) Surface morphology of a thin GaN grown on GaAs substrate and (b) cross-section of the FESEM, of which reveals the thickness of the cubic layer of $\sim 0.6 \mu\text{m}$	79
Figure 4.24:	(a) Surface morphology and (b) cross-sectional image of $\sim 5 \mu\text{m}$ cubic GaN grown on GaAs substrate. Both insets show the magnified images in higher magnification.	80
Figure 4.25 :	(a) Surface morphology and the inset shows the image in higher magnification. (b) Cross-sectional image of $\sim 50 \mu\text{m}$ cubic GaN grown on GaAs substrate.	81
Figure 4.26:	AFM 3-dimensional images of cubic GaN samples of (a) $\sim 0.6 \mu\text{m}$ (thin), (b) $\sim 5 \mu\text{m}$ (thick) and (c) $\sim 50 \mu\text{m}$ (bulk). Details inspection on the surface structure can be observed in the magnified images.	82
Figure 4.27:	XRD data of (a) $\sim 0.6 \mu\text{m}$, (b) $\sim 5 \mu\text{m}$ and (c) $\sim 50 \mu\text{m}$ cubic GaN grown GaAs substrate.	83
Figure 4.28:	PL spectra of cubic GaN layers with the thickness of (a) $\sim 0.6 \mu\text{m}$ (b) $\sim 5 \mu\text{m}$ and (c) $\sim 50 \mu\text{m}$. The inset figure shows detailed inspection of the thin cubic GaN sample.	85
Figure 4.29:	PL spectrum of cubic GaN layers with the thickness of (a) $\sim 5 \mu\text{m}$ and (b) $\sim 50 \mu\text{m}$. The dashed line shows the Gaussian fitting to the measured data.	85
Figure 4.30:	PL intensity of hexagonal GaN at $\sim 3.4 \text{ eV}$ (dashed line with full-triangle) and the estimated percentage of hexagonal inclusions (solid line with full-star) as functions of depth for a $\sim 50 \mu\text{m}$ thick cubic GaN (c-GaN). The inset figure shows the data was collected from the point near GaAs/c-GaN interface towards the surface.	88
Figure 4.31:	Raman spectrum of $\sim 0.6 \mu\text{m}$ thick cubic GaN grown on GaAs (001) substrate.	88
Figure 4.32:	Raman spectra of $\sim 5 \mu\text{m}$ and $\sim 50 \mu\text{m}$ cubic GaN grown on GaAs (001) substrate. On the right side, shows the separation of the LO modes of c-GaN and h-GaN at the peak around 740 eV . The dashed line shows the Gaussian fitting to the measured data.	89

LIST OF SYMBOLS

A	Surface area
a	Lattice constant, a
B	Magnetic field
c	Lattice constant, c
d_{hkl}	Interplanar spacing of crystal planes
E	Electric field (Hall effect related equation)
E	Young modulus (Strain related equation)
E_A	Binding energy of acceptor
E_D	Binding energy of donor
E_g	Energy bandgap
F	Applied force
I	Current
k_B	Molecular beam epitaxy
N	Sodium hydroxide
q	Near band edge
R_H	Hall coefficient
T	Temperature
t	Thickness
V	Voltage
V_h	Hall voltage
v	Carrier velocity (Hall effect related equation)
ν	Poisson ratio (Strain related equation)
W	Separation between two contact

α	Thermal coefficient
θ	Debye temperature
ε	Strain
σ	Stress
λ	Wavelength

LIST OF ABBREVIATIONS

AFM	Atomic force microscopy
CCD	Charge coupled device
DAP	Donor acceptor pair
<i>eA</i>	Free electron to acceptor
FDS	Fixed divergence slit
FESEM	Field emission scanning electron microscopy
FWHM	Full width half maximum
GaN	Gallium nitride
GaAs	Gallium arsenide
KOH	Potassium hydroxide
LO	Longitudinal optical
MBE	Molecular beam epitaxy
NaOH	Sodium hydroxide
NBE	Near band edge
NMR	Nuclear magnetic resonance
PL	Photoluminescence
PRS	Programmable receiving slit
RC	Rocking curve
RMS	Root mean square
RSM	Reciprocal space mapping
TEM	Transmission electron microscopy
TO	Transverse optical
UV	Ultraviolet

LIST OF PUBLICATIONS

1. S. N. Waheeda, N. Zainal, Z. Hassan, Role of pre-annealing treatment in improving the porosity of gallium nitride on cubic silicon (100) substrate, *Material Science in Semiconductor Processing*, Vol. 30, (2015), 330-334.
2. S. N. Waheeda, N. Zainal, Z. Hassan, S. V. Novikov, A. V. Akimov, A. J. Kent, Low fraction of hexagonal inclusions in thick and bulk cubic GaN layers, *Applied Surface Science*, Vol. 317, (2014), 1010-1014.

Conference proceeding

1. S. N. Waheeda, N. Zainal, Z. Hassan, R. E. L. Powell, A. V. Akimov, A. J. Kent, Properties of strain in GaN layer grown on Si (100) substrate and its porous structure, 2nd Meeting of Malaysia Nitrides Research Group (MNRG) 2015, Universiti Sains Malaysia. (Oral presentation)
2. S. N. Waheeda, N. Zainal, S. V. Novikov, A. V. Akimov, A. J. Kent, Z. Hassan, Existence of hexagonal inclusions in cubic GaN, National Physics Conference (PERFIK) 2014, Kuala Lumpur, Malaysia. (Oral presentation)
3. S. N. Waheeda, N. Zainal, Z. Hassan, Characterization of GaN film on Si (100) substrate, National Physics Conference (PERFIK) 2014, Kuala Lumpur, Malaysia. (Poster presentation)
4. S. N. Waheeda, N. Zainal, S. V. Novikov, A. V. Akimov, A. J. Kent, Z. Hassan, Investigation of hexagonal inclusions in thick and bulk cubic GaN, 1st Meeting of Malaysia Nitrides Research Group (MNRG) 2014, Universiti Sains Malaysia. (Oral presentation)

FABRIKASI DAN PENCIRIAN GaN YANG DITUMBUH DI ATAS KUBIK SUBSTRAT Si (100) DAN GaAs (001)

ABSTRAK

Secara umumnya tesis ini membentangkan kajian lapisan GaN yang ditumbuh di atas substrat Si (100). Pada bahagian pertama tesis ini, sifat-sifat lapisan GaN di atas substrat kubik Si telah dibincangkan. Penambahbaikan ke atas sifat-sifat lapisan GaN telah dikesan melalui kaedah penyepuhlindapan. Melalui pengukuran morfologi, struktur dan optik, suhu optimum bagi penyepuhlindapan ialah sekitar 800 °C. Kemudian, eksperimen punaran foto-elektrokimia dijalankan untuk fabrikasi lapisan mikrometer berliang ke atas lapisan GaN tersebut. Kesan penyepuhlindapan pada suhu optimum seterusnya dikaji ke atas sifat-sifat GaN berliang. Ciri-ciri GaN berliang dikaji melalui pemerhatian sifat morfologi, kristalografi dan optikal. Sebagai perbandingan kepada pra- disepuh lindap berliang GaN, dua lagi sampel GaN berliang juga disediakan, 1) tanpa penyepuhlindapan dan 2) dengan penyepuhlindapan selepas fabrikasi berliang. Berdasarkan pemerhatian, didapati bahawa hasil proses pra-penyepuhlindapan dalam pembentukan liang GaN adalah lebih baik serta meningkatkan kualiti kristal berbanding sampel GaN berliang yang lain. Selain itu, dari sudut optikal, sampel pra- disepuh lindap berliang GaN menunjukkan sifat pendarkilau yang lebih baik daripada sampel-sampel lain. Dapatan kajian daripada bahagian pertama telah diguna pakai dalam bahagian kedua kajian ini, yang memberi tumpuan kepada penyiasatan kewujudan kemasukan heksagon dengan mengesan kecacatan susunan dalam kubik GaN yang ditumbuh di atas (001) berorientasikan GaAs kubik substrat. Kecacatan susunan adalah mekanisme utama yang menggalakkan kewujudan bahan fasa heksagonal, yang seterusnya merendahkan kualiti kristal dan ketulenan sampel GaN kubik. Kesalahan susunan dan kemasukan

GaN heksagon adalah lebih tinggi apabila ketebalan kubik GaN meningkat. Dapatan kajian mendapati bahawa kecacatan susunan dalam sampel pukal kubik GaN (~50 μm) hilang disebabkan faktor penghapusan dan peratusan heksagon GaN adalah kurang daripada 22%. Walau bagaimanapun, butiran pengukuran PL menunjukkan kandungan kemasukan heksagonal hanya beberapa peratus pada lapisan kubik GaN ~10 μm yang pertama. Hal ini menjadikannya sebagai permukaan yang baik untuk pertumbuhan kubik nitrida yang berikutnya. Dalam kajian ini, kami telah membuktikan bahawa kekonduksian sampel kubik GaN berbeza mengikut ketebalan hasil daripada jumlah kemasukan heksagon serta kecacatan dan kekotoran pada tahap yang berbeza. Walau bagaimanapun, sifat elektrik yang berkaitan dengan keboleherakan Hall dan kepekatan pembawa perlu diperbaiki untuk meningkatkan prestasi peranti berkuasa tinggi.

FABRICATION AND CHARACTERIZATION OF GaN GROWN ON CUBIC Si (100) AND GaAs (001) SUBSTRATES

ABSTRACT

In general, this thesis presents the study of GaN layer grown on different cubic substrates. In the first part of this work, the properties of GaN film grown on (100)-oriented cubic Si substrate was investigated. Improvement in the properties of the GaN layer are observed by means of thermal annealing treatment. From the morphological, structural and optical measurements, the optimum annealing temperature was found to be around 800 °C. Next, a photo-electrochemical etching technique was setup to fabricate a porous layer onto the GaN layer. The effect of thermal annealing at optimum annealing temperature is further studied on the properties of the porous GaN samples. The characteristics of the porous GaN were then investigated by observing its morphology, crystallography and optical properties. For comparison to the porous GaN, which was annealed prior to the etching (pre-annealed), another two porous GaN samples are also prepared, 1) without the annealing and 2) with the post-annealing. Based on the observations, it was found that the pre-annealing treatment results in a better formation of porous GaN while its crystalline quality is improved than its counterparts. Besides, from the optical point of view, the pre-annealed porous GaN still shows better luminescence properties among all. The outputs from the first part has been adopted in the second part of this work, which mainly focussed on investigating the presence of the hexagonal inclusions by detecting the evidence of stacking faults in the cubic GaN grown on (001)-oriented cubic GaAs substrate. Such faulty mechanism favored the growth of hexagonal phase materials, which in turn degrades the crystalline quality and purity of the cubic samples. The stacking faults and the hexagonal GaN inclusions increased as the thickness of the cubic GaN is

higher. It was found that the stacking faults disappeared in bulk cubic GaN sample (~50 μm) due to the annihilation factor and the percentage of hexagonal GaN was less than 22 %. However, the hexagonal inclusions was just few percent in the first ~10 μm layer of the cubic GaN. It appears to be a better surface for the subsequent cubic nitrides growth. Apart from that, it was revealed that the conductivity of cubic GaN samples varied with thickness as a result of different amount of hexagonal inclusions as well as defects and impurities level. Nonetheless, the electrical properties related to the Hall mobility and carrier concentration need to be improved to increase the performance of high power devices.

CHAPTER 1:

INTRODUCTION

Gallium nitride (GaN) has been spotted as a preferable material for high powerful devices, mainly due to its direct and wide band gap material that allows its devices to work at high temperature operation, high power and high frequency devices. Despite of that, huge demands on high quality GaN layers remains desirable. At present, GaN is commercially grown on sapphire (Al_2O_3) substrate and the lattice mismatched between both materials is $\sim 16\%$. The use of the Al_2O_3 substrate in the GaN based devices always leads to complicated fabrication processes, whereby sidewall lithography etching technique is required to allow vertical transport throughout the device structure since sapphire is an insulator material. In addition to that, poor thermal conductivity of Al_2O_3 as compared to Si precludes efficient dissipation of heat produced by GaN-based high current devices.

Therefore, growing GaN layers on Si substrate is one of the ways to reduce the device fabrication cost. However, such heteroepitaxial growth tends to promote higher threading dislocations and cracks as compared to sapphire substrate. These issues lead to degradation of efficiency of GaN-based devices. Up to now, various methods and techniques are employed in order to minimize the threading dislocation densities and other strains in GaN layer grown on Si substrate. In common practice, a low temperature AlN buffer layer is grown prior to the GaN layer to ameliorate the problems. Yet, the effect of the threading dislocations and strains cannot be completely removed. There is report revealed that thermal annealing is a direct way to improve the properties of the GaN layer grown on Si substrate by partially removing the defects density such as threading dislocations inside the layer [1].

It is worth noting that porous structure is an alternative strategy to further reduce the defects and strains [2] while enhancing the extraction of the trapped light as in light emitting diodes (LEDs) due to the total internal reflection. Nevertheless, one of the critical issues to produce porous GaN nowadays is the surface of the pores tends to damage during the etching process and without careful control, the entire nitride layer might be ‘wiped-out’. After the etching, the unwanted non-stoichiometric conditions; either Ga- or N-rich surface is formed, which somehow causes broadening in the XRD peak. Works by Vajpeyi et al. [3] and Hartono et al. [4] demonstrated that the thermal annealing helped to restore the quality of the porous GaN after being damaged by the etching process. This process is called post-annealing treatment. However, such treatment may reduce the pores density and distort the pores shape, especially if the sample was annealed at very high temperature. Therefore, in this work, we propose a new technique to improve the quality of porous GaN by annealing the GaN sample prior to the etching process (called pre-annealing treatment). Details of this work will be given in Chapter 4. Apart from that, strain and stress generation in the GaN layers are investigated. This is a crucial study as both contribute to the imperfections in the GaN material. It is important to note that the study of properties of hexagonal GaN grown on cubic Si (100) substrate is to provide an idea for the second part of this work, which will focus on detecting hexagonal GaN inclusions inside cubic GaN grown on GaAs (001) substrate.

It should be noted that most GaN based devices are grown under thermodynamically stable hexagonal (wurtzite) structure. Nonetheless, the efficiency of the optoelectronic devices such as laser and light emitting diodes (LEDs) is limited by the high presence of piezoelectric and spontaneous polarization fields [5]. Therefore, growing the GaN devices in cubic (zinc-blende) structure will help to

eliminate the fields due to the absence of spontaneous polarization field in the non-polar materials. In addition to that, cubic GaN offers easy cleavage along its substrate facet and has high carrier mobility (especially holes due to higher crystal symmetry). Nevertheless, the main issue in cubic GaN epitaxy is that the hexagonal GaN phase material always incorporates in the cubic growth since the cubic material is a metastable structure in nature [6]. Such inclusions affect the purity of the cubic GaN and impair its potential to be adopted in wide range of device applications. In cubic GaN, the main defect is coming from stacking faults [7]. This faulty is closely related to the existence of hexagonal inclusions inside cubic structure, which then alters the cubic stacking sequences. For this reason, we aim at reducing the amount of the hexagonal inclusions, especially at higher thickness of cubic GaN.

In general, the scope of this work covers the properties of both hexagonal and cubic GaN layers grown on different cubic substrate. The outlines of this work are based on the objectives, as follow:

- i) To investigate the properties of hexagonal GaN layer grown on cubic Si (100) substrate.
- ii) To improve the properties of GaN layer grown on cubic Si (100) substrate by means of thermal annealing and porous fabrication.
- iii) To determine the presence of hexagonal inclusions in cubic GaN layers grown on GaAs (001) substrate with different thickness.

This thesis is organized as follows:

Chapter 2 describes the basic properties of GaN material and some background research related to the growth, fabrication and characterization of GaN material.

Chapter 3 provides the growth technique and characterization tools used to grow and evaluate the properties of GaN layers. The explanation on the thermal annealing process and the setup for the porous fabrication technique are also given.

Chapter 4 presents data and analysis on GaN layers grown on Si (100) and GaAs (001) substrates. At the beginning, the properties of GaN on Si (100) are discussed by means of its morphological, crystallographical and optical aspects. Next, the effects of annealing and porous fabrication on GaN layer are also studied in this work. Meanwhile, investigations on analysis of cubic GaN on GaAs (001) substrate at thin, thick and bulk thickness will be presented. Here, we aimed at observing the existence of the amount of hexagonal inclusions in cubic GaN samples.

Chapter 5 concludes the findings of this work and highlights the potential of the GaN samples to be adopted in the future device applications. Besides, some suggestion and opinions on the related future works are provided as the efforts to improve the current research project.

CHAPTER 2:

THEORY AND LITERATURE REVIEW

This chapter describes basic knowledge and reviews on reported works of gallium nitride (GaN) material. Basically, GaN exists in both hexagonal (wurtzite) and cubic (zinc-blende) structures. Therefore, different structure provides different lattice parameter of which leads to different fundamental properties of nitride materials. The stress and strain effect as well as the formation of defects in the GaN material would limit the performance of the material for devices. In an attempt to reduce the strain and defects in the GaN material, thermal treatment and porous fabrication process have been demonstrated by some researchers. Reviews on published works on cubic GaN is also included in this chapter, focusing on the growth of cubic GaN and amount of hexagonal inclusions.

2.1: Introduction to GaN material

It is undeniable that the GaN material has brought a great impact to advancements in semiconductor devices today due to its direct and wide band gap of ~3.46 eV. It is even more interesting if GaN material is combined with In and Al to form an alloy, as this could cover the emission from the whole visible spectrum. Despite of those feasible technological applications of GaN, growing high quality GaN is still a big challenge due to the non-availability of GaN substrate. So, the GaN material has to be grown on foreign substrates. As a result to the reliability on the heteroepitaxial growth, most of GaN layers suffer from high strain and defects, generated from the non-lattice matched system between GaN and the foreign substrate. Therefore, a proper optimized growth conditions need to be figured-out. Besides, a

better understanding on the defects formation during the growth is important so that their impact to the GaN based devices can be minimized. Typical defects that exist in GaN material will be discussed in the next section.

2.2: Basic properties of GaN material

GaN commonly exists in the form of hexagonal (wurtzite) structure. This is due to the thermodynamically stable phase of the structure. On the other hand, GaN material in cubic (zinc-blende) structure is a metastable in nature, whereby its epitaxy remains challenging until today. In the hexagonal close-packed (hcp) unit, there are two lattice parameters¹, which commonly denotes as a and c . Meanwhile in cubic, the atoms are arranged in equal distance with high crystal symmetry (so-called face-centered cubic (fcc)), meaning that a cubic unit cell has a single lattice constant, a . Each atom in both system is tetragonally coordinated with four atoms of different species. Figure 2.1 describes the atomic arrangement of hexagonal and cubic GaN. Both crystal structures differ only in term of their stacking sequence. As illustrates in figure 2.2, the stacking sequence of the hcp in hexagonal structure is ABABAB whereas the cubic structure is ABCABC [8].

¹ Lattice parameter also known as lattice constant that refers to the physical dimension of a unit cell in a crystal structure.

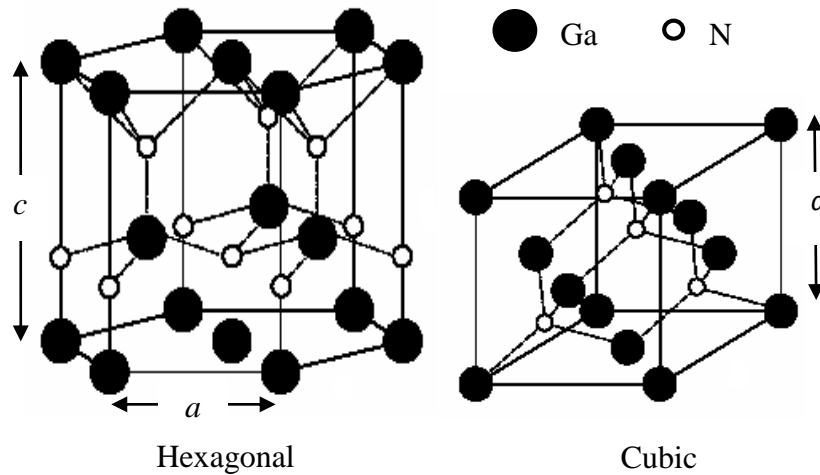


Figure 2.1: The atomic arrangement in hexagonal (wurtzite) and cubic (zinc-blende) GaN materials.

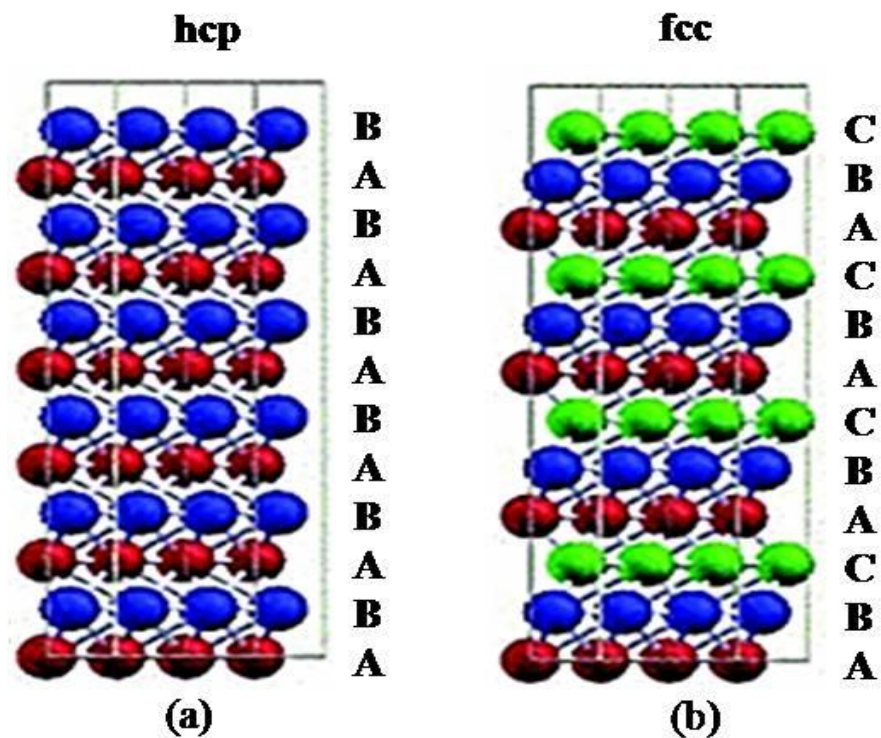


Figure 2.2: Stacking sequence of (a) hexagonal and (b) cubic lattice.

Table 2.1 represents the basic properties of the GaN material in both hexagonal and cubic structure. In term of thermal stability, hexagonal GaN is more stable than cubic GaN. For this reason, growing hexagonal and cubic GaN requires different growth conditions. In the case of cubic GaN, the growth process is more challenging

and needs certain approach to obtain high purity cubic GaN sample due to its metastable nature. Theoretically, the lattice constants of both structures are shown as below. However, the lattice constants are highly affected by the amount of strain inside the material [9]. If the lattice constant is smaller than the theoretical value, it experiences compressive strain. If otherwise, tensile strain will be expected. It can also be seen that the energy band gap is getting lower when temperature increases. This is due to the ‘shrinking’ of bandgap at higher temperature, as been stated in [10]. From physical appearance, GaN is a transparent and hard material and it has relatively high melting point.

Table 2.1: Basic properties of both hexagonal and cubic GaN.

Properties	Hexagonal GaN	Cubic GaN
Structure	Wurtzite	Zinc-blende
Stability	Stable	Metastable
Lattice constant at 300 K	$a_o = 0.3189$ nm $c_o = 0.5185$ nm	0.450 nm
Energy Gap, E_g	Direct	Direct
Energy Gap, E_g at 300 K	3.46 eV [11]	
Energy Gap, E_g at 6 K		3.27 eV [12]
Energy Gap, E_g at 0 K	3.50 eV [13]	3.30 eV [13]
Melting point	2773 K [14]	2770 K [14]
Hardness at 300K	15.5 ± 0.9 GPa [14]	

2.3: Type of defects exist in the growth of GaN material

Growing GaN in a perfect crystal structure still hypothetical since the generation of defects inside the material during the growth is unavoidable. However, with latest technology in epitaxial growth, the presence of the defects can be minimized. This section will classify and explain the type of defects such as threading

dislocations, stacking faults and vacancies, which are commonly found in most GaN materials.

2.3.1: Threading dislocations: Screw and edge dislocations in GaN

Dislocation in semiconductor material is a commonly known as a line defect. Dislocation defines the imperfection or distortion in a crystal and it can be divided into two types; 1) screw dislocation and 2) edge dislocation. Their mechanisms are illustrated in Figure 2.3. During the movement of the atomic lattices, the dislocations allow slip while plastic deformation occurs when the inter-atomic bonds are fractured and reformed. Nonetheless, the dislocations lower the stress by allowing the slip. Throughout the slipping process of one plane, it creates dislocations that propagate across the crystal. The lattice distortion caused by the dislocations is explained by Burgers vector, b , which describes the size and the direction of the distortion. Note that in real situation, a semiconductor material could have the mixture of dislocations of the screw and edge.

It is worth noting that the dislocations density in a semiconductor material can be estimated through x-ray diffraction (XRD) measurement. Based on some reviews, the dislocation density of GaN lies within the range of 10^8 - 10^{10} cm^{-2} . According to the Rosner et al. [15], threading dislocations are likely to be the center of non-radiative recombinations that somehow will degrade the device performance. Besides that, report by Wong et al. [16] revealed the threading dislocations are not only affecting the optical behavior of the GaN material but also the structural and electrical aspects. The presence of threading dislocations will cause a broadening of the XRD peak. On the other hand, in term of electrical properties, the electron mobility seems to be more affected by the presence of the edge dislocation compared to the screw dislocation.

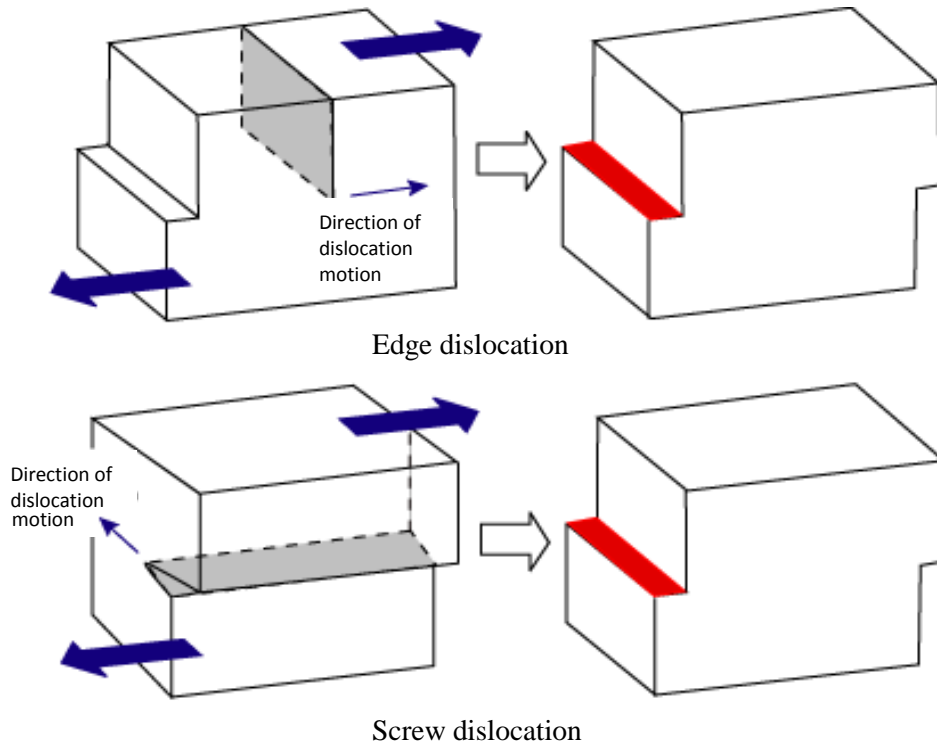


Figure 2.3: Mechanism of edge and screw dislocations in a semiconductor material [17].

2.3.2: Stacking faults in GaN material

Stacking fault is categorized as a planar defect. It is said to occur when there is an interruption in the stacking sequence of a crystal lattice, as been shown in Figure 2.4. The effect of the stacking faults gives significant degradation of purity in cubic GaN material. As been described before, cubic GaN has the atomic sequence in ABCABC. Due to the presence of the stacking faults, the sequence can be easily interrupted. This faulty leads to the formation of hexagonal phase material inside the cubic GaN. Therefore, the stacking faults have been regarded as the main factor contributes to the existence of hexagonal GaN material in cubic GaN. According to the previous report by Tsuchiya et al. [18], the hexagonal GaN inclusions increase when the cubic GaN was grown at higher thickness. Moreover, surface roughness is always related to the existence of the hexagonal inclusions in cubic GaN. It is important to note that, the evidence of stacking faults disappears in a very thick nitride

layer. This is due to the annihilation mechanism that occurs when two stacking faults, which are lying on $\{111\}$ planes, intersect and annihilate each other. This explains why large amount of defects confined near the interface of the materials. Moreover, this implies that the density of stacking faults is independent to the amount of hexagonal inclusions. Further discussions on the results will be discussed in the Chapter 4.

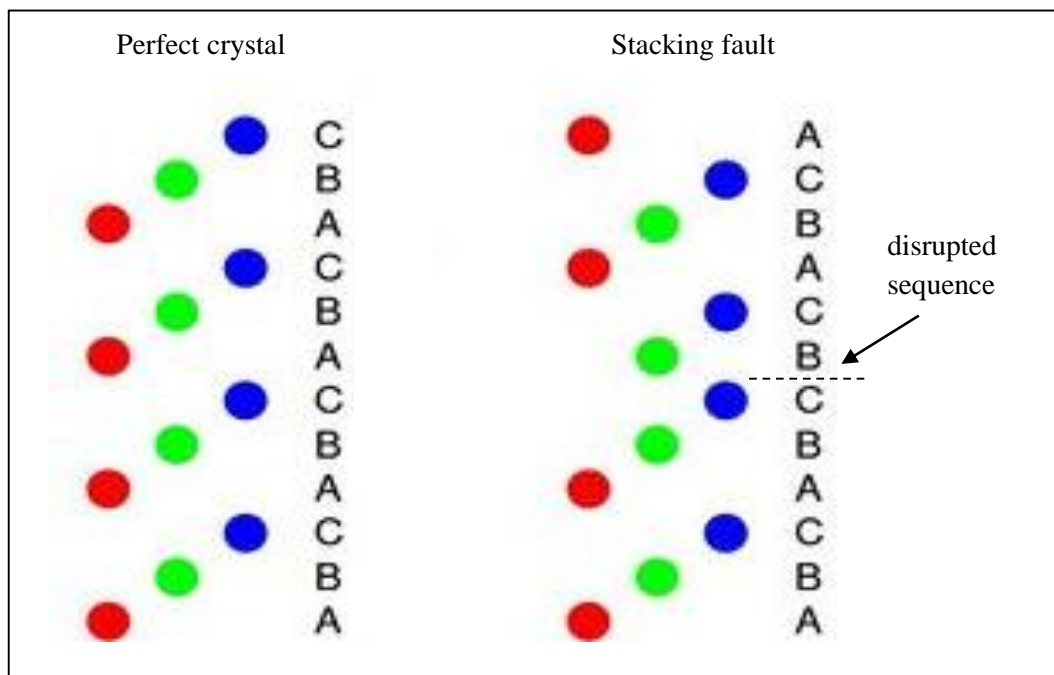


Figure 2.4: Disrupted sequence in the stacking fault phenomenon.

2.3.3 Vacancy in GaN material

Vacancy is a type of point or zero-dimensional defects, which can be divided into two categories; intrinsic and extrinsic defects. The intrinsic defects occur when there is a missing atom left a vacancy site in the lattice structure. On the other hand, the extrinsic defects refers to the substitution occupied foreign atoms into the lattice sites, so-called substitutional in the crystal lattice. This case is applied to the intentionally added atoms. If the present atom is unwanted, we called it as impurity.

These phenomenons are illustrated in Figure 2.5. In this work, the evidence of defects related vacancies in GaN is observed through photoluminescence measurement. The defects normally produce yellow luminescence in the spectrum. The vacancies include $V_{\text{Ga}}\text{O}_{\text{N}}$ complexes. The V_{Ga} refers to gallium vacancy while O_{N} refers to the substitutional of oxygen atom at the nitrogen sites [19].

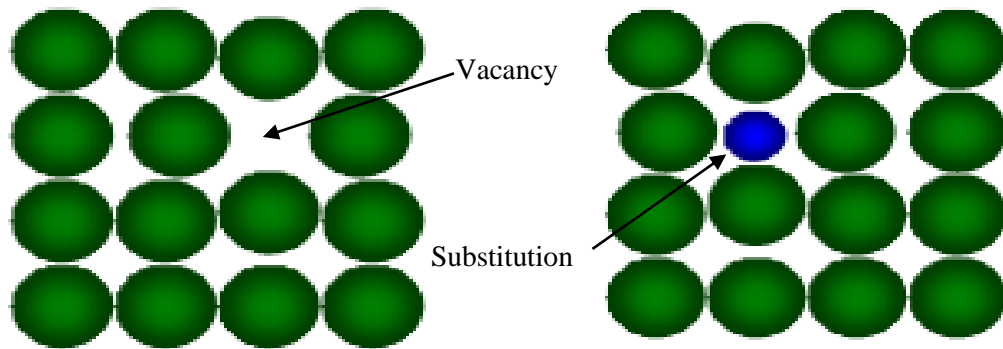


Figure 2.5: Illustration of vacancy and substitutional defects in lattice structure.

2.3.4: Strain and stress mechanism

In semiconductor material, strain is the change in shape or size (or deformation) of the material when an external force is applied. Meanwhile, stress refers to the internal force per unit area associated to the strain. The stress, σ can be explained by the equation below:

$$\sigma = \frac{F}{A} \quad (2.1)$$

where F refers to the applied force and A is the area. The deformation of the material or strain, ε is described as below:

$$\varepsilon = \frac{\Delta L}{L_0} \quad (2.2)$$

where, ΔL refers to the length stretched or compressed whereas L_0 is the initial length of the material as shown in Figure 2.6.

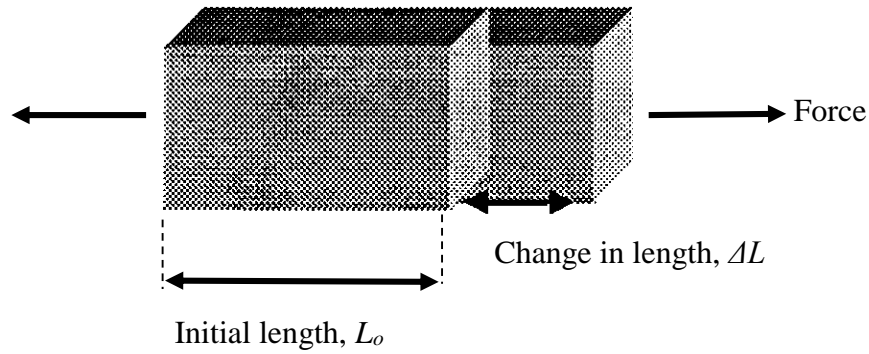


Figure 2.6: Illustration of deformation of the object under an applied force [19].

Figure 2.7 explains the mechanism of compressive and tensile stress in relation to the growth of a semiconductor material on the same substrate or different substrate. When the material is grown on the same substrate material, this is called homoepitaxial. Normally, the material will be grown in nearly perfect structure as the lattice parameters of both are equal. However, GaN is typically grown on foreign substrates (so-called heteroepitaxial) since the GaN substrate is still missing in the market. It should be beared in mind that different materials have different value of lattice parameters. This creates a lattice mismatch system of the growth. As a result, the GaN layer may experience mechanical stress, either in compressive or in tensile, in order to conform the lattice structure of the GaN to the substrate. Such condition will induce the formation of interfacial defects; e.g. misfit dislocations during the interaction of the atomic lattice. Eventhough misfit dislocation is only a point defect but it could serve as a platform for the defects to propagate towards the GaN surface. Thus, this limits the potential of the GaN layer to be fabricated into working devices.

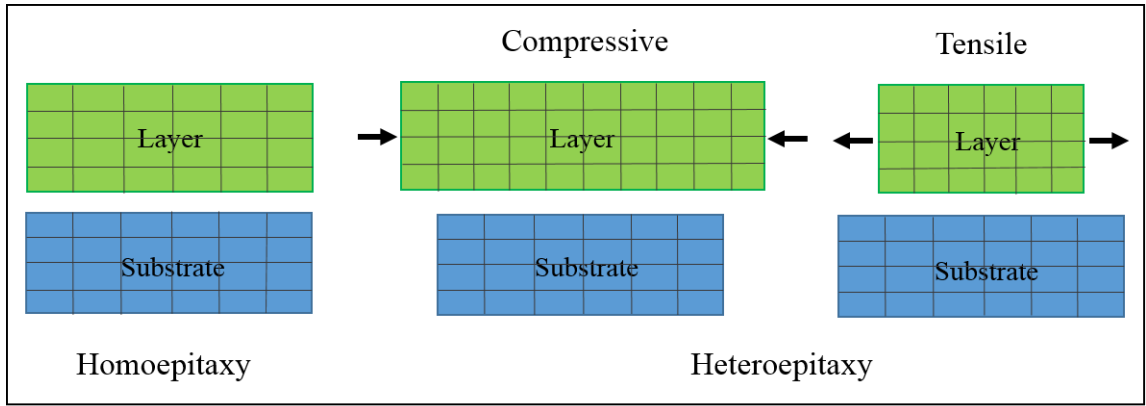


Figure 2.7: Illustration of lattice matched and lattice mismatched mechanism in epitaxy.

2.4: Progress in GaN epitaxy

As been mentioned earlier, the growth of GaN usually takes place on foreign substrates due to the non-availability of commercial GaN substrate to run homoepitaxial growth. Sapphire (Al_2O_3) and silicon (Si) are two common substrates used to grow GaN. As comparison, sapphire is more expensive with respect to Si. For this reason, Si is considered as the preferable substrate for GaN, especially in mass production level. However, it should be highlighted that the GaN layer grown on Si substrate always suffers from high defects density and cracks due to large difference in lattice constant and thermal expansion coefficient between both materials [20]. This constraints the efforts of using the GaN layer for further applications. As an attempt to minimize the problem, many researchers have proposed to introduce a buffer layer or insertion layer prior to the GaN growth as to mediate the lattice constants between the GaN material and the foreign substrates. Such layer serves to reduce the impact of the defects density and strain to the GaN layer.

Table 2.2 summarizes earlier published works on the growth of GaN using different substrates, with various use of the buffer layers. In early 90s, Nakamura had proposed the growth of GaN on GaN buffer layer [21]. This work suggested the

optimum thickness of GaN buffer layer to be around 20 nm. On the other hand, Zhao et. al [22] investigated the effect of using AlN buffer layer at different thickness in the GaN growth. The thickness was varied between 16 to 45 nm. They found that the GaN sample with the AlN buffer layer of 20 nm thick showed the highest reduction in the FWHM. From the works, the optimum thickness of both GaN and AlN buffer layers is similar. However, from the results [23, 24], the GaN buffer layer gives better results in term of the crystalline and electrical properties. Note that, in the case of growing GaN layer on Si substrate, GaN is not a preferable buffer layer due to large difference in the lattice parameters of both materials. Besides, growing GaN directly on Si is difficult as it tends to create a wetting problems condition due to the difference in its surface energies. Therefore, 3C-SiC and AlN have been proposed as the buffer layer for the growth of GaN on Si substrate. Even so, the AlN buffer layer is widely used than the SiC buffer layer as the SiC layer tends to promote amorphous structure to the GaN. Furthermore, it received less attention as the SiC substrate is costly, which make it impracticable for mass production purpose. Note that AlN serves a smaller difference in the lattice mismatch to GaN, which around 2.5% [25]. Besides, the use of AlN as a buffer layer also helps in the reduction of tensile stress in the grown samples, as been observed in [26, 27]. Earlier work by Eric et al. [28] proposed a superlattice structure in an attempt to achieve a relaxed GaN layer. Further improvement in the GaN crystalline quality was obtained by increasing the number of superlattices in the GaN structure. Nevertheless, growing superlattices structure is very complex and challenging as to maintain uniformity of each grown layer. After all, the AlN buffer still becomes the most convenient and practical way in growing a better quality of GaN layers.

Table 2.2: Comparison of the growth of GaN on different buffer layer and substrate.

Substrate	Proposed layer	Dislocation density (cm ⁻²)	Remarks	Reference
Al ₂ O ₃	GaN buffer layer			Nakamura [21]
	AlN buffer layer			Zhao et. al [22]
Si	3C-SiC buffer layer	10 ⁸ -10 ⁹		Masayoshi et. al [23]
	AlN buffer layer	9×10 ⁹		Zhang et. al [24]
	GaN/AlN superlattices		<ul style="list-style-type: none"> - FWHM decreases with higher number of superlattices - Relaxed GaN obtained 	Eric et al. [28]
	LT-AlN insertion layer		<ul style="list-style-type: none"> - Tensile stress decreases 	Zhang et al. [26]
	AlN buffer layer		<ul style="list-style-type: none"> - FWHM decreases at thicker buffer layer (up to 80 nm) - Relaxation of tensile strain towards thicker buffer layer 	Kim et al. [27]
SiC	AlN buffer layer			Ding et. al [29]

2.5: Thermal annealing treatment on GaN

Thermal annealing is a heat treatment that allows the alteration of the surface morphology, optical as well as electrical properties of the GaN layer. The optimum annealing temperature differs, depending on the materials used. The applied heat in this treatment provides the energy to the atoms to recrystallize in a better structure and progresses toward the equilibrium state. Such movement during the process helps to redistribute and exterminate the dislocations in the crystal structure. And so, the thermal annealing is one of the post-treatment that commonly applied in the growth of GaN layer, regardless of their growth method and conditions.

2.5.1: Role of thermal annealing in improving GaN

In this section, some survey on the published works related to the use of annealing temperature towards improving the quality of GaN material have been performed. The details are summarized in Table 2.3. For example, Zhu et al. [30] revealed that the annealing temperature above 800 °C will degrade the structural quality of the sample and Chang et al. [31] have applied the same temperature to improve the optical properties of their sample. In fact, Kelly et al. [32] have reported that the annealing temperature above 900 °C will cause broadening in the XRD peak and surface roughness. On the other hand, Jhin et al. [33] found that the optimum annealing temperature in their work to be ~900 °C. However, further increase in the annealing temperature showed a degradation of crystalline quality while an increase in the biaxial stress inside their samples. The effect of thermal annealing on the strain relaxation in GaN sample was studied. In most cases, the crystalline quality of the sample is better when it is subjected to the annealing. Based on these findings, we have applied the temperature of 800 °C to anneal our GaN sample. The related results on this subject will be presented in Chapter 4. Note that, different works will provide different optimum annealing temperature, yet it still serves for the reduction of stress in the GaN layer, as been proved in the earlier works [33]

Table 2.3: Summary of some published works on annealing GaN at various temperature.

Working annealing temperature	Remarks	Reference
800 °C, 900°C, 1000°C	A slight increase in the FWHM (obtained by XRD) for annealing temperature > 800 °C - indicate material degradation	Zhu et al. [30]
800 °C	Annealing at different condition with constant temperature	Chang et al. [31]
900 °C, 1000 °C, 1100 °C, 1200 °C, 1300 °C	FWHM and surface roughness increase at annealing temperature > 900 °C	Kelly et al. [32]
700 °C , 800 °C, 900 °C, 1000 °C	Annealing GaN at 900 °C shows highest reduction in FWHM value	Jhin et al. [33]
850°C	Annealed GaN samples show smaller FWHM value with respect to the non-annealed -tensile strain decreases for annealed GaN samples	Wu et al. [34]

2.6: Background study of porous fabrication on GaN layer

Porous structure is an alternative method to reduce the strain in a GaN sample. There are few works have adopted a superlattice structure prior to the GaN growth in order to promote strain relaxation [28, 35]. However, this method is quite complicated in maintaining the optimum structure of the superlattice before the GaN can be grown. It should be noted that porous GaN layer is not only offering a means for strain relaxation condition [4] but also helps to ‘drain-out’ the threading dislocations from propagating into the next layers. Besides, porous GaN has a high surface to volume ratio and shows improvement in optical properties [36], which make it a suitable structure for advanced sensor and optical devices.

With the development in nanostructure technology, many researchers established the fabrication of porous structure. This structure can be obtained through various etching procedures, which can be categorized into dry etching and wet etching

techniques. There are several dry etching techniques of which involves ion-assisted mechanisms such as ion milling [37], chemical assisted ion beam etching (CAIBE) [38], reactive ion etching (RIE) [39] and inductively-coupled plasma reactive ion etching (ICP-RIE) [40]. However, the dry etching techniques are quite costly and lead to severe damage on the surface without careful control in parameters. On the other hand, the wet etching technique, for example photo-electrochemical (PEC) etching offers low surface damage [41], cheaper and simpler process compared to the conventional dry etching techniques. Earlier works related to the fabrication of porous GaN using photo-electrochemical etching are reviewed here and discussion are given follows.

A work by Mynbaeva et al. [42] reported that the reduction of stress is in one magnitude lower in porous GaN sample as compared to the non-porous GaN sample. It is well known that GaN grown on sapphire substrate exhibits high influence of compressive stress due to the lattice mismatched system. However, , the amount of compressive stress was reduced in the porous GaN layer, fabricated by Vajpeyi et al. [43]. Based on the observations, they proposed that the fabrication of porous GaN helps to release strain in the GaN layer. Apart from reducing the amount of stress, porous GaN structure also shows better properties in optical aspect [36, 43, 44]. Summary of the results are presented in Table 2.4.

Table 2.4: Data from published works on the crystalline quality and stress relaxation by the fabrication of the porous GaN prepared by different conditions.

Substrate	Crystalline quality	Strain and stress condition	Reference
SiC		$\sigma_a = +0.04$	Mynbaeva et al. [42]
Al ₂ O ₃	FWHM of E ₂ (high) of porous GaN decreases with respect to non-porous GaN	Relaxation of compressive stress by ~0.25 GPa in porous GaN sample	Vajpeyi et al. [43]
	FWHM of the XRD measurement decreases	Red shifted towards stress-free GaN	Hartono et al. [36]
-		Strain relaxed layer is proposed	Hartono et al. [4]
	FWHM of E ₂ (high) for all porous GaN decrease with respect to non-porous GaN	Stress relaxation increases with etching duration	Al-Heuseen et al. [44]

Based on the findings, we acknowledge that both annealing and porous fabrication are able to promote strain reduction in the GaN sample. Yet, there still lack of published works report on the effect of annealing on porous GaN structure. Up to now, only few works [3, 45] had applied the annealing treatment to the porous structure after the etching. However, the GaN porosity may increase further if the porous GaN was annealed prior to the etching. Details discussion will be provided in Chapter 4.

2.7: Progress on the growth of cubic GaN

Much research in recent years has focused on hexagonal GaN, instead of cubic GaN. It is well known that GaN is naturally crystallized in the hexagonal structure, which in fact contains strong piezoelectric and spontaneous polarization fields induced by variation of strains. The effect of the internal fields would limit the performance of optoelectronic devices. In order to solve this issue, growing GaN in cubic structure will be free from the internal fields. Despite of this, growing cubic GaN is much more challenging due to the metastable nature of the cubic material that allows the co-

existence of hexagonal GaN phase materials. To address this problem, growth parameters like III/V growth ratio, growth temperature and growth rate must be optimized to maintain the cubic growth. According to a report in [46], the growth of GaN tends to promote 3-D islands growth at high temperature. In addition to that, growing cubic GaN by MBE technique requires a relatively low temperatures; typically below ~ 700 °C, in contrast to MOVPE system that operates at temperature above 900 °C. If the temperature is too high upon the MBE growth, the decomposition rate of the Ga and N atoms from the surface will be higher. Such decomposition will affect the quality of the GaN epitaxial layer. Meanwhile, for the cubic GaN growth by MOCVD or MOVPE, there are few works focussed on the properties of cubic GaN with variation of V/III ratio. As been observed in [58], the percentage of cubic contents decreased significantly outside the optimum V/III ratio, which indicates that the growth of cubic phase was disrupted either under the N-rich or Ga-rich conditions. Later, more extreme investigations on the effect of V/III ratio to the cubic GaN growth was conducted by MOVPE [60]. They found that the low V/III ratio is the best condition as to achieve high quality cubic GaN. In principle, the growth of cubic GaN should be conducted under the stoichiometric condition, however, a slightly Ga-rich condition is crucial as to maintain and improve the cubic growth regardless of their growth method. The Ga-rich condition helps to reduce the surface energy, which will facilitate the cubic GaN growth. Previous works reported on the growth details of GaN layer are summarized in Table 2.5.

Table 2.5: Growth parameters used for growing cubic GaN layers by various groups.

Growth method	Growth temperature (°C)	N ₂ flow rate (sccm)	NH ₃ flow rate	Ga flux	N/Ga flux ratio	Reference
MBE	720				0.5 - 1.0	Lima et al. [47]
	680 - 720	1				Katayama et al. [48]
	400 - 700	3				Chen et al. [49]
	600-650					Brandt et al. [50]
	720 - 835					As et al. [51]
	620 - 680				3.0 x 10 ¹³ - 1.5 x 10 ¹⁴ atoms/cm ²	Yang et al. [52]
	600 - 700	3				Liu et al. [53]
	630	2				Balakrishnan et al. [54]
	750					Kemper et al. [55]
	720				4.4 x 10 ¹⁴ atoms/cm ²	Schormann et al. [56]
MOCVD	850		17 860 μmol/min	15 μmol/min		Zheng et al. [57]
	750 - 985				600 - 2500	Wei et al. [58]
	530 - 600		1 slm	8.9 μmol/min	3000	Hong et al. [59]
MOVPE	900 - 950				1000 - 20000	Onuma et al. [60]
	940			18 μmol/min		Nagayama et al. [61]

2.7.1: Hexagonal inclusions in cubic GaN

Earlier report by Tsuchiya et al. [62] on the growth of thick cubic GaN on GaAs (100) revealed the absence of hexagonal inclusions at its optimum growth temperature of 900 °C with V/III ratio of 600 at its lowest growth rate. Upon increasing the growth rate while decreasing V/III ratio, the GaN growth showed the mixture of cubic and hexagonal phase materials. After that, they proposed another work [63] on growing cubic GaN, using different substrate of GaAs (001). In this work, the hexagonal inclusions were found to be less than 1% for cubic layer below than 2 μm thick. This result was only obtained under the V/III ratio of 200. Note that, the hexagonal percentage will increase exponentially with the increase in the growth time [63], which subsequently affected the growth rate as well. Such increment in the hexagonal inclusions caused by rough surface, especially at higher thickness. Again, another report on the cubic GaN by Sun et al. provides the similar hexagonal GaN diffraction of $(10\bar{1}1)$ while the hexagonal percentage for the samples found to be around 1.6 - 7.9 % [64]. In the following year, Qu et al. [65] reported the amount of hexagonal inclusions from the diffraction of $(10\bar{1}0)$ and $(10\bar{1}1)$ was found to be around 2.76 %. Much works have been published on cubic GaN but only few reports on the amount of hexagonal inclusions in their samples. The amount of hexagonal contents was estimated from the XRD measurements. It should be noted that the percentage of the hexagonal inclusions will be more at higher thickness as the difficulty to maintain the cubic growth over long period. In addition, T. Onuma et al. [60] had revealed that the XRD intensity of cubic GaN improved while the hexagonal GaN signal suppressed at low V/III ratio. A high amount of hexagonal inclusions of 78 % was reported in [55, 66]. This is most probably due to the substrate patterning

that formed the {111} faceted surface, which then favored the formation of hexagonal inclusions inside the cubic GaN.

Besides that, there is lack of report on the properties of cubic GaN, especially at higher thickness. Most of the cubic growth at higher thickness would prefer HVPE technique. However, such technique applies high growth rate that will affect the cubic growth. In this work, our cubic samples were grown by MBE, including the thicker layer. We will discuss the properties of cubic GaN grown at different thickness up to ~50 μm thick, by focusing on the amount of hexagonal inclusions in the cubic samples.

Table 2.6: Hexagonal inclusions in cubic GaN grown by different technique.

Growth technique	Thickness of c-GaN (μm)	Observed XRD diffraction		h-GaN inclusions (%)	Reference
		c-GaN	h-GaN		
HVPE	5	(200) (400)	-		Tsuchiya et al. [62]
HVPE	-	(002)		< 1	Tsuchiya et al. [63]
MOVPE	2	(002)	($\bar{1}\bar{1}01$)		Nagayama et al. [67]
MOCVD	-	(002)	($10\bar{1}1$)	1.6 - 7.9	Sun et al. [64]
MOCVD	-	(002)	($10\bar{1}0$) ($10\bar{1}1$)	~2.76	Qu et al. [65]
MOVPE	1.2	(002)	(0002) ($10\bar{1}1$)		Onuma et al. [60]
MBE	1.4	(002)	($\bar{1}011$)		Kemper et al. [55]

2.8: Summary

Descriptions on the basic properties and reviews on previous works related to the hexagonal and cubic GaN have been discussed in this chapter. Such reviews provide us an insight to further improve the properties of the GaN layer through